

Algebraic Multiscale Method for one-dimensional elliptic problems

Kanghun Cho*, Roktaek Lim[†], Dongwoo Sheen[‡]

Thursday 27th January, 2022

Abstract

In this paper we propose an idea of constructing a macro-scale matrix system given a micro-scale matrix linear system. Then the macro-scale system is solved at cheaper computing costs. The method uses the idea of the generalized multiscale finite element method based. Some numerical results are presented.

Keywords. Multiscale, algebraic multiscale method, heterogeneous coefficient.

1 Introduction

In this paper we propose an algebraic multiscale method for one-dimensional elliptic problems. The extension to two dimensional case will appear in [3].

Assume that only the algebraic information on the components of a micro-scale linear system are known, but no further information on the coefficient κ and the source term f are available. In this situation, our object is to try to construct macro-scale linear systems using accessible information and find numerical solutions which possess similar properties of the solutions obtained by multiscale methods. In some sense, this is an inverse problem to fetch the necessary information on the fast-varying coefficient and the source function of governing elliptic equation. This will give us elliptic equation in micro-scale. Then, we follow the standard approach to build a macro-scale linear system based on a multiscale method. Although other multiscale methods can generate similar macro-scale linear systems, in this paper we use the generalized multiscale finite element method approach.

*Samsung Fire & Marine Insurance Co., Ltd., 14, Seocho-daero 74-gil, Seocho-gu, Seoul 06620, Korea;

[†]Department of Biology, Hong Kong Baptist University, Cha Chi-ming Science Tower, Ho Sin Hang Campus, Kowloon Tong, Hong Kong

[‡]Department of Mathematics, Seoul National University, Seoul 08826, Korea
Emails:serein@snu.ac.kr, rokt.lim@gmail.com, sheen@snu.ac.kr

Multiscale methods have been actively developed in various manners including heterogeneous multiscale methods [1, 2], multiscale hybridizable discontinuous Galerkin methods [4, 7, 8], and multiscale finite element methods [6, 9, 10]. Here we adopt the generalized multiscale finite element method(GMsFEM) [5, 11].

The generalized multiscale finite element spaces consist of snapshot function spaces, offline function spaces, and moment function spaces. First, snapshot functions are obtained by solving κ -harmonic problems in each macro element. Then offline functions are constructed by applying suitable dimension reduction techniques to snapshot function space. We choose offline functions identical to snapshot function space since there are only two snapshot functions in each macro element.

This paper is organized as follows. In section 2, we briefly review the non-conforming generalized multiscale finite element method(GMsFEM) based on DSSY finite element space. Then the algebraic multiscale method for two-dimensional elliptic problem is introduced in section 3 following the framework of GMsFEM. Section 4 is devoted to energy norm error estimate of the proposed method. In Section 5, representative numerical results are presented. A conclusion is given in Section 6.

2 Preliminaries

In this paper, we consider the following one-dimensional elliptic problem:

$$\begin{cases} -\frac{d}{dx}\left(A\frac{du}{dx}\right) = f \text{ in } \Omega, \\ u = 0, \text{ if on } \partial\Omega, \end{cases} \quad (2.1)$$

where $\Omega = (0, 1)$, $\partial\Omega = \{0, 1\}$, and A is a rapidly varying coefficient. Denote by $(\mathcal{T}_H)_{0 < H < 1}$ and $(\mathcal{T}_h)_{0 < h < 1}$ two families of macro and micro-scale triangulations of $(0, 1)$ into macro and micro-scale subintervals such that $0 = X^0 < X^1 < \dots < X^{N_H} = 1$ and $0 = x_0 < x_1 < \dots < x_{N_h} = 1$. Here, and in what follows, H and h stand for the macro and micro-scale mesh parameters given by

$$H = \max_{K=1, \dots, N_H} (X^K - X^{K-1}), \quad h = \max_{j=1, \dots, N_h} (x_j - x_{j-1}).$$

We assume that $\{X^0, X^1, \dots, X^{N_H}\} \subset \{x_0, x_1, \dots, x_{N_h}\}$ and $h \ll H < 1$. For $K = 1, \dots, N_H$, denote by H^K the size of K -th macro interval $I^K = (X^{K-1}, X^K)$. Let $\{x_j^K\}_{j=0}^{N^K}$ be the set of nodes for the macro interval $I^K = (X^{K-1}, X^K)$ and designate by I_j^K the j -th subinterval (x_{j-1}^K, x_j^K) with length h_j^K for $j = 1, \dots, N^K$ such that $x_0^K = X^{K-1}$ and $x_{N^K}^K = X^K$. For each K , let $\{\phi_j^K\}_{j=0, \dots, N^K}$ be the space of standard basis functions for the C^0 -piecewise linear finite element space on the interval $I^K = (X^{K-1}, X^K)$. Denote by Ψ_{\pm}^K the macro-scale basis function in the interval I^K , which can be obtained as the

solutions of

$$\begin{cases} -\frac{d}{dx}\left(A\frac{d}{dx}\Psi_-^K\right) = 0 \text{ in } I^K, \\ \Psi_-^K(X^{K-1}) = 1, \Psi_-^K(X^K) = 0, \end{cases} \quad (2.2)$$

and

$$\begin{cases} -\frac{d}{dx}\left(A\frac{d}{dx}\Psi_+^K\right) = 0 \text{ in } I^K, \\ \Psi_+^K(X^{K-1}) = 0, \Psi_+^K(X^K) = 1. \end{cases} \quad (2.3)$$

For each K let us seek $\Psi_{h,\pm}^K$ which approximate Ψ_{\pm}^K in the form

$$\Psi_{h,-}^K = \sum_{j=1}^{N^K-1} \eta_{j,-}^K \phi_j^K + \phi_0^K, \quad (2.4a)$$

$$\Psi_{h,+}^K = \sum_{j=1}^{N^K-1} \eta_{j,+}^K \phi_j^K + \phi_{N^K}^K. \quad (2.4b)$$

Since $\Psi_{h,\pm}^K$ are piecewise-linear in I^K , one may set

$$\frac{d}{dx}\Psi_{h,\pm}^K = \gamma_{j,\pm}^K \text{ in } I_j^K \text{ for some constant } \gamma_{j,\pm}^K, j = 1, \dots, N^K. \quad (2.5)$$

Assuming that $\frac{1}{A(x)} \in L^1(a, b)$, one sees that the exact solution of the differential equation

$$\begin{cases} -\frac{d}{dx}\left(A\frac{dw}{dx}\right) = 0, \text{ in } (a, b) \\ w(a) = 0, w(b) = 1. \end{cases}$$

is given by

$$w(x) = \beta \int_a^x \frac{1}{A(s)} ds \quad a.e. x \in (a, b), \quad (2.6)$$

where β is the harmonic mean of $A(x)$ over (a, b) , i.e.,

$$\beta = \frac{1}{\int_a^b \frac{1}{A(s)} ds}. \quad (2.7)$$

Thanks to (2.6) and (2.7), it is easy to see that

$$\Psi_-^K(x) = \frac{\int_x^{X^K} \frac{1}{A(s)} ds}{\int_{X^{K-1}}^{X^K} \frac{1}{A(s)} ds} \text{ for all } x \in I^K, \quad (2.8a)$$

$$\Psi_+^K(x) = \frac{\int_{X^{K-1}}^x \frac{1}{A(s)} ds}{\int_{X^{K-1}}^{X^K} \frac{1}{A(s)} ds} \text{ for all } x \in I^K. \quad (2.8b)$$

Denote an n -dimensional vector with parameters K and \pm as follows:

$$\boldsymbol{\alpha}_{\pm}^K = (\alpha_{1,\pm}^K, \dots, \alpha_{n,\pm}^K)^t \in \mathbb{R}^n.$$

Recalling (2.4), (2.5), and (2.8), and utilizing the principle of energy norm minimization of finite element method, we deduce the following equalities:

$$\begin{aligned}
& \min_{\boldsymbol{\eta}_+^K \in \mathbb{R}^{N^K}} \left\{ \int_{I^K} A(x) \left[\frac{d}{dx} (\Psi_+^K(x) - \Psi_{h,+}^K(x)) \right]^2 dx \right\}^{\frac{1}{2}} \\
&= \min_{\boldsymbol{\eta}_+^K \in \mathbb{R}^{N^K}} \sum_{j=1}^{N^K} \left\{ \int_{I_j^K} A(x) \left[\frac{d}{dx} (\Psi_+^K(x) - \Psi_{h,+}^K(x)) \right]^2 dx \right\}^{\frac{1}{2}} \\
&= \min_{\gamma_+^K} \sum_{j=1}^{N^K} \left\{ \int_{I_j^K} A(x) \left(\frac{\beta}{A(x)} - \gamma_{j,+}^K \right)^2 dx \right\}^{\frac{1}{2}} \\
&= \min_{\gamma_j^K} \sum_{j=1}^N \left\{ \int_{I_j^K} \left(\frac{\beta^2}{A(x)} - 2\beta\gamma_{j,+}^K + A(x)(\gamma_{j,+}^K)^2 \right) dx \right\}^{\frac{1}{2}}.
\end{aligned}$$

After differentiating the above with respect to γ_j^K , we have

$$\gamma_{j,+}^K = \frac{\int_{x_{j-1}^K}^{x_j^K} \beta dx}{\int_{x_{j-1}^K}^{x_j^K} A(x) dx} = \frac{\beta h_j^K}{\int_{x_{j-1}^K}^{x_j^K} A(x) dx}.$$

If $A(x) = 1$, $\gamma_j^K = 1$.

3 Algebraic Multiscale Method

In this section, we introduce an algebraic multiscale method. Assume that we are given a linear system:

$$\mathbf{A}^h \boldsymbol{\eta}^h = \mathbf{b}^h, \tag{3.1}$$

which is obtained by a discretization of a micro-scale elliptic equation of form (2.1). Assuming that the coefficient A and the source function f are not known directly, our aim is to construct a macro-scale matrix system

$$\mathbf{A}^H \boldsymbol{\eta}^H = \mathbf{b}^H \tag{3.2}$$

from the micro-scale linear system (3.1). In particular, without solving the macro-scale basis problem (2.2) for each macro element I^K , we try to infer the components of \mathbf{A}^H and \mathbf{b}^H which are obtained by a multiscale method from the structure of the elliptic problem (2.1). Then the macro-scale linear system (3.2) is solved at a cheaper cost.

From now on, the midpoint rule is assumed to approximate integrals.

We state the algorithm as follows, and describe the details in the subsections to follow.

Step 1. Approximate the coefficients and RHS of (2.1) from the micro-scale matrix system;

Step 2. Construct a macro-scale matrix system from the information obtained in Step 1;

Step 3. Solve the macro-scale matrix system to get a multiscale solution.

3.1 Micro-scale problem

Let $\{\phi_j\}_{j=0,\dots,N_h}$ be the space of standard basis functions for the C^0 -piecewise linear finite element space on $\Omega = (0, 1)$. We have

$$\left. \frac{d\phi_j}{dx} \right|_{[x_{j-1}, x_j]} = \frac{1}{h_j} \text{ and } \left. \frac{d\phi_j}{dx} \right|_{[x_j, x_{j+1}]} = -\frac{1}{h_{j+1}}, \quad (3.3)$$

where h_j is the size of j -th micro interval $I_j = (x_{j-1}, x_j)$. Let A^h be the micro-scale stiffness matrix. For $1 \leq j \leq N_h - 1$, the diagonal element of A^h is given as follows:

$$\begin{aligned} [A^h]_{j,j} &= \int_{x_{j-1}}^{x_{j+1}} A(x) \frac{d\phi_j}{dx} \frac{d\phi_j}{dx} dx \\ &= \int_{x_{j-1}}^{x_j} A(x) \left(\frac{1}{h_j}\right)^2 dx + \int_{x_j}^{x_{j+1}} A(x) \left(-\frac{1}{h_{j+1}}\right)^2 dx \\ &\approx \frac{1}{h_j} A_{j-\frac{1}{2}} + \frac{1}{h_{j+1}} A_{j+\frac{1}{2}}. \end{aligned} \quad (3.4)$$

For $j = 0$ and $j = N_h$,

$$[A^h]_{0,0} \approx \frac{1}{h_1} A_{\frac{1}{2}}, \quad [A^h]_{N_h, N_h} \approx \frac{1}{h_{N_h}} A_{N_h - \frac{1}{2}}. \quad (3.5)$$

The off-diagonal element of A^h can be computed similarly:

$$[A^h]_{j,j-1} \approx -\frac{1}{h_j} A_{j-\frac{1}{2}}, \quad [A^h]_{j,j+1} \approx -\frac{1}{h_{j+1}} A_{j+\frac{1}{2}}. \quad (3.6)$$

From above equation, we know that there is an one-to-one correspondence between the off-diagonal element of A^h and the average of coefficient matrix in each micro interval.

To compute the right hand side b^h , we assume $f = \frac{dg}{dx}$ for some $g \in H^1(\Omega)$. Since the derivatives of micro-scale basis functions are piecewise constant functions, it makes the computation simpler. For $1 \leq j \leq N_h - 1$,

$$\begin{aligned} b_j^h &= \int_{x_{j-1}}^{x_{j+1}} f \phi_j dx = \int_{x_{j-1}}^{x_j} \frac{dg}{dx} \phi_j dx + \int_{x_j}^{x_{j+1}} \frac{dg}{dx} \phi_j dx \\ &= [\phi_j g]_{x_{j-1}}^{x_j} - \int_{x_{j-1}}^{x_j} \frac{d\phi_j}{dx} g dx + [\phi_j g]_{x_j}^{x_{j+1}} - \int_{x_j}^{x_{j+1}} \frac{d\phi_j}{dx} g dx \\ &= g(x_j) - \int_{x_{j-1}}^{x_j} \frac{1}{h_j} g dx - g(x_j) + \int_{x_j}^{x_{j+1}} \frac{1}{h_{j+1}} g dx \\ &\approx g(x_{j+\frac{1}{2}}) - g(x_{j-\frac{1}{2}}). \end{aligned} \quad (3.7)$$

For $j = 0$ and $j = N_h$,

$$b_0^h = g(x_{\frac{1}{2}}) - g(x_0), \quad b_{N_h}^h = g(x_{N_h}) - g(x_{N_h - \frac{1}{2}}). \quad (3.8)$$

Under the additional assumption $f = \frac{dg}{dx}$, there are only $N_h + 1$ equations (3.7), (3.8) to decide $N_h + 2$ unknowns $g(x_0), g(x_{\frac{1}{2}}), g(x_{\frac{3}{2}}), \dots, g(x_{N_h - \frac{1}{2}}), g(x_{N_h})$. Thus these unknowns are computed up to an additive constant, which corresponds to the constant of indefinite integration. Hence we further assume that

$$g(x_0) = 0, \quad (3.9)$$

From (3.7)–(3.9) it follows that

$$g(x_0) = 0; \quad g(x_{j+\frac{1}{2}}) = \sum_{k=0}^j b_k^h, \quad j = 0, \dots, N_h - 1, \quad g(x_{N_h}) = \sum_{k=0}^{N_h} b_k^h. \quad (3.10)$$

3.2 Macro-scale problem

Let $\{\Psi^K\}_{I=0}^{N_H}$ be a set of macro-scale basis functions on $\Omega = (0, 1)$. For $1 \leq K \leq N_H - 1$, Ψ^K satisfies the equations:

$$\begin{cases} -\frac{d}{dx}\left(A\frac{d}{dx}\Psi^K\right) = 0 \text{ in } I^K, \\ \Psi^K(X^{K-1}) = 0, \quad \Psi^K(X^K) = 1, \end{cases} \quad (3.11)$$

and

$$\begin{cases} -\frac{d}{dx}\left(A\frac{d}{dx}\Psi^K\right) = 0 \text{ in } I^{K+1}, \\ \Psi^K(X^K) = 1, \quad \Psi^K(X^{K+1}) = 0. \end{cases} \quad (3.12)$$

Thus

$$A\frac{d}{dx}\Psi^K = \begin{cases} c^K & \text{a.e. in } I^K, \\ c^{K+1} & \text{a.e. in } I^{K+1}, \end{cases}$$

where c^K and c^{K+1} are constants. Assume that $\frac{1}{A(x)} \in L^1(a, b)$. Integrating $\frac{d}{dx}\Psi^K = c^K/A(x)$ over I^K gives

$$1 = c^K \int_{X^{K-1}}^{X^K} \frac{dx}{A(x)}.$$

That is,

$$A\frac{d}{dx}\Psi^K = \frac{1}{\int_{X^{K-1}}^{X^K} \frac{dx}{A(x)}} \text{ on } I^K.$$

Similarly,

$$A\frac{d}{dx}\Psi^K = -\frac{1}{\int_{X^K}^{X^{K+1}} \frac{dx}{A(x)}} \text{ on } I^{K+1}.$$

Let A^H be the macro-scale stiffness matrix. For $1 \leq K \leq N_H - 1$, the diagonal element of A^H is given as follows:

$$\begin{aligned}
[A^H]_{K,K} &= \int_{X^{K-1}}^{X^{K+1}} A(x) \frac{d\Psi^K}{dx} \frac{d\Psi^K}{dx} dx \\
&= \frac{1}{\int_{X^{K-1}}^{X^K} \frac{dx}{A(x)}} \int_{X^{K-1}}^{X^K} \frac{d\Psi^K}{dx} dx - \frac{1}{\int_{X^K}^{X^{K+1}} \frac{dx}{A(x)}} \int_{X^K}^{X^{K+1}} \frac{d\Psi^K}{dx} dx \\
&= \frac{1}{\int_{X^{K-1}}^{X^K} \frac{dx}{A(x)}} + \frac{1}{\int_{X^K}^{X^{K+1}} \frac{dx}{A(x)}}. \tag{3.13}
\end{aligned}$$

For $K = 0$ and $K = N_H$,

$$[A^H]_{0,0} = \frac{1}{\int_{X^0}^{X^1} \frac{dx}{A(x)}}, \quad [A^H]_{N_H, N_H} = \frac{1}{\int_{X^{N_H-1}}^{X^{N_H}} \frac{dx}{A(x)}}. \tag{3.14}$$

The off-diagonal element of A^H can be computed similarly:

$$[A^H]_{K, K-1} = -\frac{1}{\int_{X^{K-1}}^{X^K} \frac{dx}{A(x)}}, \quad [A^H]_{K, K+1} = -\frac{1}{\int_{X^K}^{X^{K+1}} \frac{dx}{A(x)}}. \tag{3.15}$$

3.3 Algebraic formulation of macro-scale system

We can construct a macro-scale matrix system from the micro-scale matrix system. Denote by M_K the number of fine nodes on $(0, X^K)$. Then

$$\begin{aligned}
\int_{X^{K-1}}^{X^K} \frac{dx}{A(x)} &= \sum_{j=1}^{N^K} \int_{x_{j-1}^K}^{x_j^K} \frac{dx}{A(x)} \approx \sum_{j=1}^{N^K} \frac{h_j}{A(x_{j-\frac{1}{2}}^K)} \\
&= \sum_{j=1}^{N^K} \frac{h_j}{A_{M_{K-1}+j-\frac{1}{2}}} = -\sum_{j=1}^{N^K} \left([A^h]_{M_{K-1}+j, M_{K-1}+j-1} \right)^{-1}. \tag{3.16}
\end{aligned}$$

Thus the off-diagonal element of A^h can be computed by

$$[A^H]_{K, K-1} = -\frac{1}{\int_{X^{K-1}}^{X^K} \frac{dx}{A(x)}} \approx \frac{1}{\sum_{j=1}^{N^K} \left([A^h]_{M_{K-1}+j, M_{K-1}+j-1} \right)^{-1}}, \tag{3.17}$$

and

$$[A^H]_{K, K+1} = -\frac{1}{\int_{X^K}^{X^{K+1}} \frac{dx}{A(x)}} \approx \frac{1}{\sum_{j=1}^{N^{K+1}} \left([A^h]_{M_K+j, M_K+j-1} \right)^{-1}}. \tag{3.18}$$

We can compute the diagonal element of A^h by the same way. For $1 \leq K \leq N_H - 1$,

$$[A^H]_{K,K} = \frac{1}{\int_{X^{K-1}}^{X^K} \frac{dx}{A(x)}} + \frac{1}{\int_{X^K}^{X^{K+1}} \frac{dx}{A(x)}} \tag{3.19}$$

$$\approx -\frac{1}{\sum_{j=1}^{N^K} \left([A^h]_{M_{K-1+j}, M_{K-1+j-1}} \right)^{-1}} - \frac{1}{\sum_{j=1}^{N^{K+1}} \left([A^h]_{M_{K+j}, M_{K+j-1}} \right)^{-1}}.$$

For $K = 0$ and $K = N_H$,

$$\begin{aligned} [A^H]_{0,0} &= \frac{1}{\int_{X^0}^{X^1} \frac{dx}{A(x)}} \approx -\frac{1}{\sum_{j=1}^{N^0} \left([A^h]_{j,j-1} \right)^{-1}}, \\ [A^H]_{N_H, N_H} &= \frac{1}{\int_{X^{N_H-1}}^{X^{N_H}} \frac{dx}{A(x)}} \approx -\frac{1}{\sum_{j=1}^{N^{N_H}} \left([A^h]_{M_{N_H-1+j}, M_{N_H-1+j-1}} \right)^{-1}}. \end{aligned}$$

Thus we can construct the macro-scale stiffness matrix only using the micro-scale stiffness matrix elements.

For the right hand side, note that

$$\begin{aligned} \int_{X^{K-1}}^{X^K} f \Psi^K dx &= \sum_{j=1}^{N^K} \int_{x_{j-1}^K}^{x_j^K} \frac{dg}{dx} \Psi^K dx = \sum_{j=1}^{N^K} \left([\Psi^K g]_{x_{j-1}^K}^{x_j^K} - \int_{x_{j-1}^K}^{x_j^K} \frac{d\Psi^K}{dx} g dx \right) \\ &= g(x_N^K) - \sum_{j=1}^{N^K} \int_{x_{j-1}^K}^{x_j^K} \frac{1}{A(x)} \frac{1}{\int_{X^{K-1}}^{X^K} \frac{dx}{A(x)}} g dx \\ &\approx g(x_N^K) - \frac{1}{\int_{X^{K-1}}^{X^K} \frac{dx}{A(x)}} \sum_{j=1}^{N^K} h_j \frac{g(x_{j-\frac{1}{2}}^K)}{A(x_{j-\frac{1}{2}}^K)}. \end{aligned}$$

Thus for $1 \leq K \leq N_H - 1$,

$$\begin{aligned} b_K^H &= \int_{X^{K-1}}^{X^{K+1}} f \Psi^K dx = \int_{X^{K-1}}^{X^K} f \Psi^K dx + \int_{X^K}^{X^{K+1}} f \Psi^K dx \\ &\approx \left(g(x_N^K) - \frac{1}{\int_{X^{K-1}}^{X^K} \frac{dx}{A(x)}} \sum_{j=1}^{N^K} h_j \frac{g(x_{j-\frac{1}{2}}^K)}{A(x_{j-\frac{1}{2}}^K)} \right) \\ &\quad + \left(-g(x_N^K) + \frac{1}{\int_{X^K}^{X^{K+1}} \frac{dx}{A(x)}} \sum_{j=1}^{N^{K+1}} h_{j+1} \frac{g(x_{j-\frac{1}{2}}^{K+1})}{A(x_{j-\frac{1}{2}}^{K+1})} \right) \\ &= \frac{1}{\int_{X^K}^{X^{K+1}} \frac{dx}{A(x)}} \sum_{j=1}^{N^{K+1}} h_{j+1} \frac{g(x_{j-\frac{1}{2}}^{K+1})}{A(x_{j-\frac{1}{2}}^{K+1})} - \frac{1}{\int_{X^{K-1}}^{X^K} \frac{dx}{A(x)}} \sum_{j=1}^{N^K} h_j \frac{g(x_{j-\frac{1}{2}}^K)}{A(x_{j-\frac{1}{2}}^K)} \\ &= \frac{1}{\sum_{j=1}^{N^{K+1}} \left([A^h]_{M_{K+j}, M_{K+j-1}} \right)^{-1}} \sum_{j=1}^{N^{K+1}} \frac{g(x_{M_{K+j}-\frac{1}{2}})}{[A^h]_{M_{K+j}, M_{K+j-1}}} \\ &\quad - \frac{1}{\sum_{j=1}^{N^K} \left([A^h]_{M_{K-1+j}, M_{K-1+j-1}} \right)^{-1}} \sum_{j=1}^{N^K} \frac{g(x_{M_{K-1+j}-\frac{1}{2}})}{[A^h]_{M_{K-1+j}, M_{K-1+j-1}}}. \end{aligned}$$

For $K = 0$ and $K = N_H$,

$$b_0^H = -g(x_0) + \frac{1}{\sum_{j=1}^{N^1} \left([A^h]_{j,j-1} \right)^{-1}} \sum_{j=1}^{N^1} \frac{g(x_{j-\frac{1}{2}})}{[A^h]_{j,j-1}},$$

$$b_{N_H}^H = g(x_{N_h}) - \frac{1}{\sum_{j=1}^{N^{N_H}} \left([A^h]_{M_{N_H-1}+j, M_{N_H-1}+j-1} \right)^{-1}} \sum_{j=1}^{N^{N_H}} \frac{g(x_{M_{N_H-1}+j-\frac{1}{2}})}{[A^h]_{M_{N_H-1}+j, M_{N_H-1}+j-1}}.$$

Since we know $g(x_0), g(x_{\frac{1}{2}}), g(x_{\frac{3}{2}}), \dots, g(x_{N_h-\frac{1}{2}}), g(x_{N_h})$ from the micro-scale right hand side vectors as given in (3.10), the macro-scale right hand side vector can be computed from the micro-scale matrix system.

3.4 Multiscale solution

Now we get the macro-scale matrix system using algebraic structure of micro-scale matrix system. We solve this macro-scale system to get the multiscale solution

$$u_{ms}^H = \sum_{K=0}^{N^H} \eta^K \Psi^K.$$

Note that for $1 \leq K \leq N^H - 1$,

$$\Psi^K(x) = \begin{cases} \Psi_+^K(x) & \text{for all } x \in I^K, \\ \Psi_-^{K+1}(x) & \text{for all } x \in I^{K+1}. \end{cases}$$

For $K = 0$ and $K = N_H$,

$$\Psi^0(x) = \Psi_-^0(x) \quad \text{and} \quad \Psi^{N_H}(x) = \Psi_+^{N_H}(x).$$

We already know the exact form of Ψ_{\pm}^K from (2.8). Using this form, we can compute the value of Ψ^K at each micro node with the micro-scale stiffness matrix elements. Note that for $1 \leq l \leq N^K$,

$$\begin{aligned} \int_{X^{K-1}}^{x_l^K} \frac{1}{A(s)} ds &= \sum_{j=1}^l \int_{x_{j-1}^K}^{x_j^K} \frac{dx}{A(x)} \approx \sum_{j=1}^l \frac{h_j}{A(x_{j-\frac{1}{2}}^K)} \\ &= \sum_{j=1}^l \frac{h_j}{A_{M_{K-1}+j-\frac{1}{2}}} = - \sum_{j=1}^l \left([A^h]_{M_{K-1}+j, M_{K-1}+j-1} \right)^{-1}. \end{aligned}$$

Thus

$$\Psi_+^K(x_l^K) = \frac{\sum_{j=1}^l \left([A^h]_{M_{K-1}+j, M_{K-1}+j-1} \right)^{-1}}{\sum_{j=1}^{N^K} \left([A^h]_{M_{K-1}+j, M_{K-1}+j-1} \right)^{-1}}.$$

Similarly,

$$\Psi_-^K(x_l^K) = \frac{\sum_{j=l+1}^{N^K} \left([A^h]_{M_{K-1+j}, M_{K-1+j-1}} \right)^{-1}}{\sum_{j=1}^{N^K} \left([A^h]_{M_{K-1+j}, M_{K-1+j-1}} \right)^{-1}}.$$

Now we can easily compute the value of u_{ms}^H at every micro node.

4 Numerical examples

In this section, we investigate some numerical examples to see the convergence behavior of our scheme. We take $N^h = 2^{10}$. The micro-scale solution u^h is used as a reference solution to compute error. Since u_{ms}^H and u^h are piecewise linear functions, we have, for all $1 \leq j \leq N_h$,

$$\begin{aligned} \frac{du_{ms}^H}{dx} \Big|_{[x_{j-1}, x_j]} &= \frac{u_{ms}^H(x_j) - u_{ms}^H(x_{j-1})}{h_j} = \frac{\Delta u_{ms}^H(j)}{h_j}, \\ \frac{du^h}{dx} \Big|_{[x_{j-1}, x_j]} &= \frac{u^h(x_j) - u^h(x_{j-1})}{h_j} = \frac{\Delta u^h(j)}{h_j}. \end{aligned}$$

The energy-norm error $E(u_{ms}^H)$ of u_{ms}^H is computed by

$$\begin{aligned} E(u_{ms}^H) &= \int_0^1 A(x) \left[\frac{d}{dx} (u_{ms}^H(x)) \right]^2 dx \Bigg\}^{\frac{1}{2}} = \left\{ \sum_{j=1}^{N_h} \int_{x_{j-1}}^{x_j} A(x) \left(\frac{\Delta u_{ms}^H(j)}{h_j} \right)^2 dx \right\}^{\frac{1}{2}} \\ &\approx \left\{ \sum_{j=1}^{N_h} \frac{1}{h_j} A(x_{j-\frac{1}{2}}) (\Delta u_{ms}^H(j))^2 \right\}^{\frac{1}{2}} = \left\{ \sum_{j=1}^{N_h} [A^h]_{j,j-1} (\Delta u_{ms}^H(j))^2 \right\}^{\frac{1}{2}}. \end{aligned}$$

The energy-norm $E(u_h)$ of u_h is obtained similarly. In the following examples, we compute the relative energy-norm error:

$$e_{energy}^H = \frac{E(u_{ms}^H - u^h)}{E(u^h)}.$$

4.1 Known Coefficient Case

Example 4.1. Consider the equation (2.1) with $\Omega = (0, 1)$, $f = -1$ and $A(x) = \frac{2}{3}(1+x)(1 + \cos(\frac{2\pi x}{\epsilon}))^2$, $\epsilon = \frac{1}{10}$. The homogenized solution is given by

$$u_{Hom}(x) = \frac{3}{2\sqrt{2}} \left(x - \frac{\log(1+x)}{\log 2} \right).$$

First we consider uniform micro-scale meshes. In Table 4.1, e_{energy}^H and $e_{L^2}^H$ denote the relative energy-norm and L^2 errors, respectively, of our AMS solutions. The errors are optimal. In Fig. 4.1 first multiscale basis functions Ψ^1 of Example 4.1 are shown with $N^H = 2, 4, 8, 16$, where uniform micro-scale

N^H	e_{energy}^H	Order	$e_{L^2}^H$	Order
2	5.00E-01		3.24E-01	
4	2.50E-01	1.00	6.74E-01	2.26
8	1.26E-01	0.99	1.63E-02	2.05
16	6.27E-02	1.00	4.07E-03	2.00
32	3.08E-02	1.02	9.73E-04	2.06
64	1.55E-02	0.99	2.51E-04	1.95

Table 4.1: Energy-norm and L^2 errors and reduction rates of Example 4.1 with uniform micro-scale meshes.

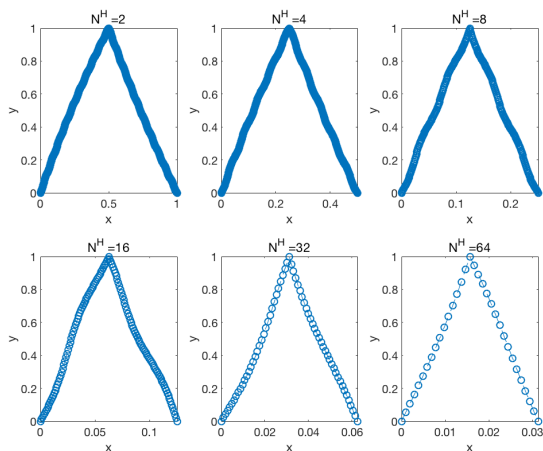


Figure 4.1: First macro-scale basis function Ψ^1 of Example 4.1 with uniform micro-scale mesh.

meshes are used. In Fig. 4.2, the red circle line and the blue dashed-cross line denote the micro-scale solution u^h and multiscale solution u_{ms}^H , respectively with $N^H = 2, 4, 8, 16, 64$. We observe that the multiscale solution u_{ms}^H converges to the micro-scale solution u^h as the size N^H becomes larger.

Next, consider non-uniform micro-scale meshes. Let $y_0 = 0$ and

$$y_{j+1} = y_j + 2 \times \frac{\text{rand}}{N_h} \text{ for } 1 \leq j \leq N_h,$$

where the MATLAB rand function is used. Take $x = \frac{y}{y_{N_h}}$ as a micro-scale mesh so that $x_{N_h} = 1$.

Tab. 4.2 shows the energy and L^2 -errors for nonuniform meshes and Figs. 4.3 and 4.4 show the graph of solutions and first multiscale basis functions. We observe that the multiscale solution u_{ms}^H converges to the micro-scale solution u^h as the size N^H becomes larger.

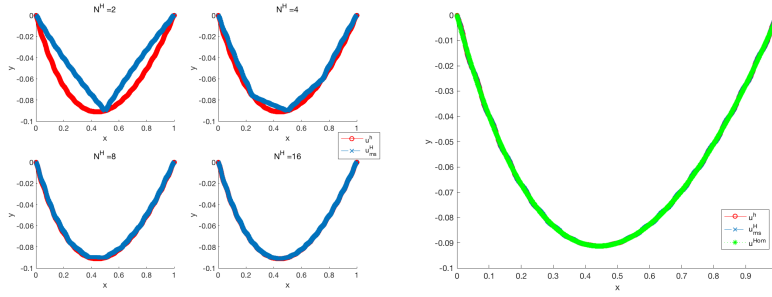


Figure 4.2: Graph of solutions of Example 4.1 with uniform micro-scale meshes: (L) with $N^H = 2, 4, 8, 16$; (R) with $N^H = 64$. \circ The red-circled and the blue dashed-cross lines denote the micro-scale solution u^h and multiscale solution u^H , respectively. The green dotted star line denotes the homogenized solution.

N^H	e_{energy}^H	Order	$e_{L^2}^H$	Order
2	5.01E-01		3.22E-01	
4	2.50E-01	1.00	6.63E-02	2.28
8	1.26E-01	0.99	1.60E-02	2.05
16	6.28E-02	1.00	4.05E-03	1.99
32	3.12E-02	1.01	9.95E-04	2.02
64	1.60E-02	0.96	2.67E-04	1.90

Table 4.2: Energy-norm and L^2 errors and reduction rates of Example 4.1 with non-uniform micro-scale meshes.

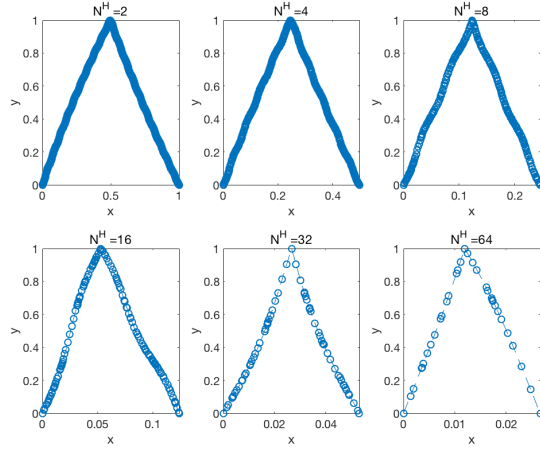


Figure 4.3: First macro-scale basis function Ψ^1 of Example 4.1 with non-uniform micro-scale mesh.

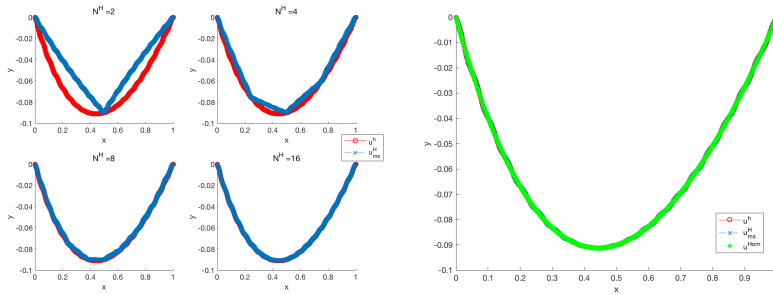


Figure 4.4: Graph of solutions of Example 4.1 with non-uniform micro-scale meshes: (L) with $N^H = 2, 4, 8, 16$; (R) with $N^H = 64$. The red-circled and the blue dashed-cross lines denote the micro-scale solution u^h and multiscale solution u_{ms}^h , respectively. The green dotted star line denotes the homogenized solution.

N^H	e_{energy}^H	Order	$e_{L^2}^H$	Order
2	5.04E-01		3.20E-01	
4	2.51E-01	1.01	6.62E-02	2.27
8	1.27E-01	0.99	1.60E-02	2.05
16	6.30E-02	1.01	3.96E-03	2.02
32	3.17E-02	0.99	9.95E-04	1.99
64	1.59E-02	1.00	2.48E-04	2.01

Table 4.3: Energy-norm and L^2 errors and reduction rates of Example 4.2.

4.2 Random Coefficient Case

We consider (2.1) with $\Omega = (0, 1)$, and the values of A and f are given randomly. That is, we consider the situation that only the micro-scale matrix system is known without any information on the exact form of A and f . Also we can further assume that we do not know the geometric information of micro-scale mesh. In our simulation, the micro-scale right hand side is given by

$$b_j^h = \text{rand for } 0 \leq j \leq N_h.$$

For the micro-scale stiffness matrix we need to infer off-diagonal elements. To construct a symmetric positive definite tridiagonal matrix A^h we use (3.4) and (3.6). We remark that the off-diagonal element of A^h corresponds to the average of coefficient matrix in each micro interval.

We consider four Examples 4.2–4.5. The cases of periodic coefficients with fixed amplitude and growing amplitude are considered in Examples 4.2 and 4.3, respectively, while those of non-periodic case in Examples 4.4 and 4.5, respectively. Error tables are given in Tabs. 4.3–4.6, and the graphs of coefficient, macro-scale basis functions, and solution graphs are shown Figs. 4.5–4.12, respectively. Notice that in particular for Example 4.4, the random coefficient leads to discontinuous macro basis functions Ψ^1 (see (3.11), (3.12)) in Fig. 4.9 and the numerical approximation by the AMS method in Fig. 4.10. Similar results are shown in Figs. 4.11–4.12. In all the cases the approach by the AMS recovers the macro-scale solutions based on the information on the micro-scale linear systems only. These solutions recover very well the macro-scale solutions obtained by the standar GMsFEM which are available when the explicit information on the coefficient $A(x)$ in micro scale and the source function $f(x)$ are known.

Example 4.2. *[Periodic behavior keeping its initial amplitude] In this example the off-diagonal elements of A^h are defined by*

$$[A^h]_{j,j-1} = (2 - 0.5 \cos(\text{rand} \times 17.7j\pi)) \text{ for } 1 \leq j \leq N_h.$$

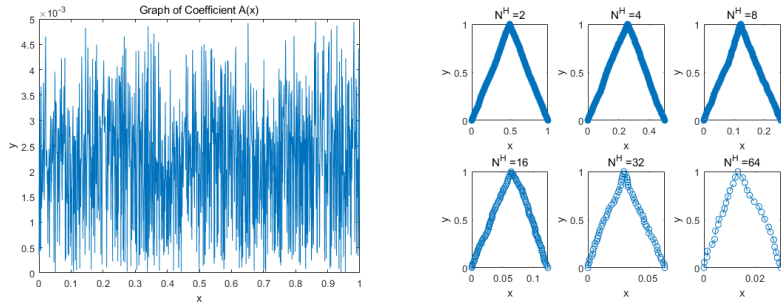


Figure 4.5: Graph of coefficient $A(x)$ of Example 4.2 and first multiscale basis functions Ψ^1 .

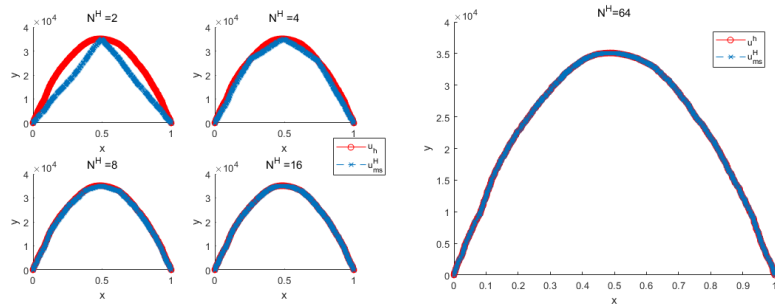


Figure 4.6: Graph of solutions of Example 4.2 with non-uniform micro-scale meshes: (L) with $N^H = 2, 4, 8, 16$; (R) with $N^H = 64$. The red-circled and the blue dashed-cross lines denote the micro-scale solution u^h and multiscale solution u_{ms}^H , respectively. The green dotted star line denotes the homogenized solution.

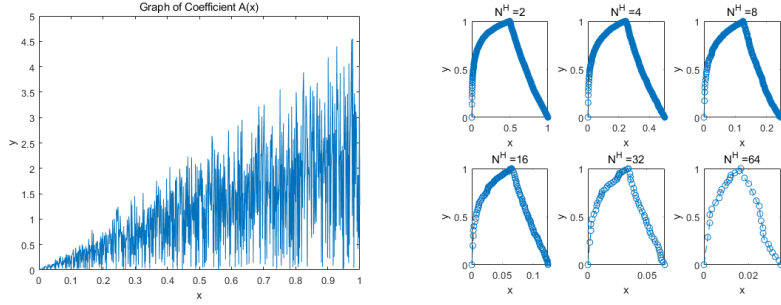


Figure 4.7: Graph of coefficient $A(x)$ of Example 4.3 and first multiscale basis functions Ψ^1 .

N^H	e_{energy}^H	Order	$e_{L^2}^H$	Order
2	5.27E-01		4.83E-01	
4	2.79E-01	0.92	1.27E-01	1.92
8	1.44E-01	0.96	3.95E-02	1.69
16	7.54E-02	0.93	1.29E-02	1.61
32	3.93E-02	0.94	4.37E-03	1.56
64	2.19E-02	0.85	1.60E-03	1.44

Table 4.4: Energy-norm and L^2 errors and reduction rates of Example 4.3.

Example 4.3. [Periodic behavior with growing amplitude] Define the off-diagonal element of A^h by

$$[A^h]_{j,j-1} = j(2 - 0.5 \cos(\text{rand} \times 17.7j\pi)) \text{ for } 1 \leq j \leq N_h. \quad (4.1)$$

Example 4.4. [Non-periodic behavior keeping its initial amplitude] Define the off-diagonal element of A^h by

$$[A^h]_{j,j-1} = \text{rand} \text{ for } 1 \leq j \leq N_h. \quad (4.2)$$

Example 4.5. [Non-periodic behavior with growing amplitude] Define the off-diagonal element of A^h by

$$[A^h]_{j,j-1} = j * \text{rand} \text{ for } 1 \leq j \leq N_h. \quad (4.3)$$

5 Conclusion

In this paper we propose to a method to compute macro-scale solutions based on the information on the linear system generated by a micro scale elliptic

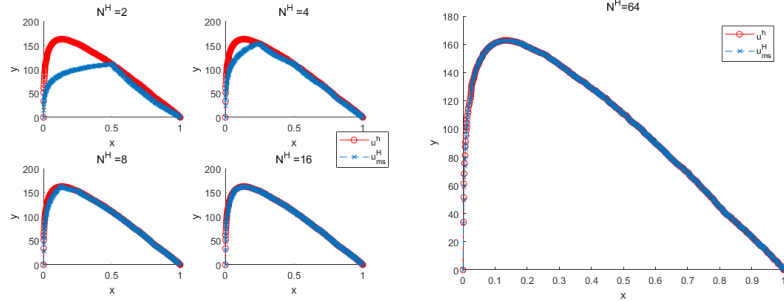


Figure 4.8: Graph of solutions of Example 4.3 with non-uniform micro-scale meshes: (L) with $N^H = 2, 4, 8, 16$; (R) with $N^H = 64$. The red-circled and the blue dashed-cross lines denote the micro-scale solution u^h and multiscale solution u_{ms}^H , respectively.

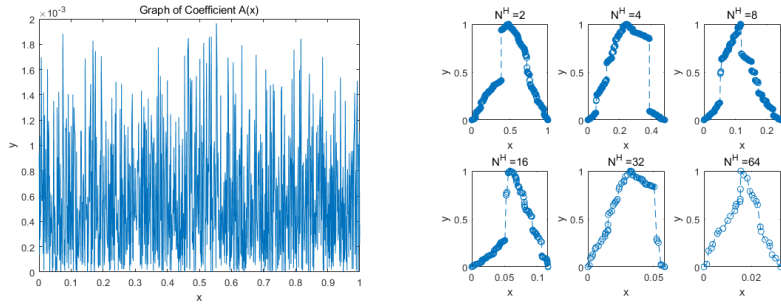


Figure 4.9: Graph of coefficient $A(x)$ of Example 4.4 and first multiscale basis functions Ψ^1 .

N^H	e_{energy}^H	Order	$e_{L^2}^H$	Order
2	5.16E-01		3.68E-01	
4	2.37E-01	1.12	5.96E-02	2.63
8	1.13E-01	1.07	1.37E-02	2.12
16	5.43E-02	1.06	3.57E-03	1.94
32	2.48E-02	1.13	6.82E-04	2.39
64	1.30E-02	0.94	2.29E-04	1.58

Table 4.5: Energy-norm and L^2 errors and reduction rates of Example 4.4.

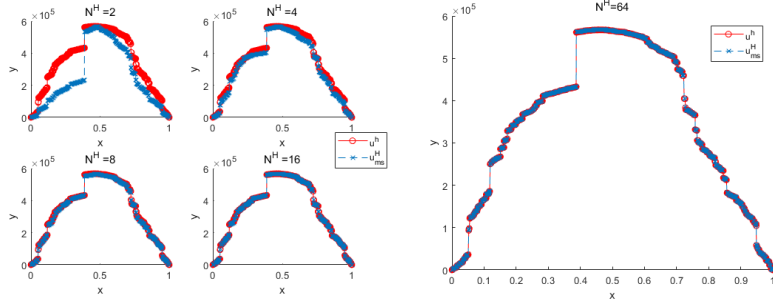


Figure 4.10: Graph of solutions of Example 4.4 with non-uniform micro-scale meshes: (L) with $N^H = 2, 4, 8, 16$; (R) with $N^H = 64$. The red-circled and the blue dashed-cross lines denote the micro-scale solution u^h and multiscale solution u_{ms}^H , respectively.

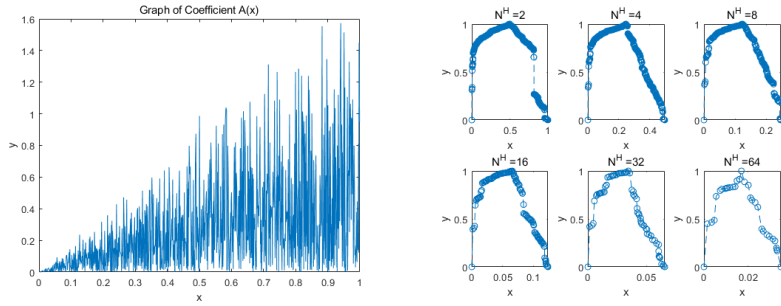


Figure 4.11: Graph of coefficient $A(x)$ of Example 4.5 and first multiscale basis functions Ψ^1 .

N^H	e_{energy}^H	Order	$e_{L^2}^H$	Order
2	4.00E-01		2.39E-01	
4	2.03E-01	0.98	6.34E-02	1.91
8	9.29E-01	1.13	1.57E-02	2.02
16	4.74E-02	0.97	5.16E-03	1.60
32	2.55E-02	0.90	2.29E-04	1.17
64	1.56E-02	0.71	1.37E-04	0.74

Table 4.6: Energy-norm and L^2 errors and reduction rates of Example 4.5.

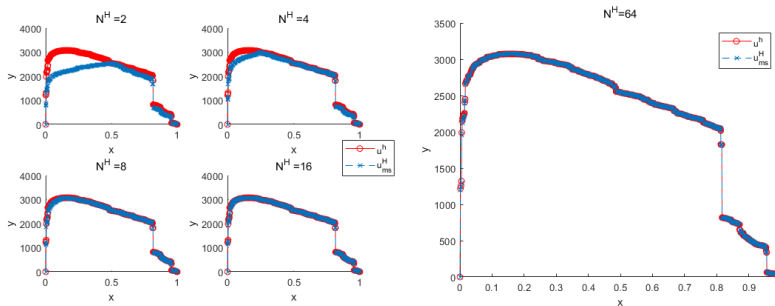


Figure 4.12: Graph of solutions of Example 4.5 with non-uniform micro-scale meshes: (L) with $N^H = 2, 4, 8, 16$; (R) with $N^H = 64$. The red-circled and the blue dashed-cross lines denote the micro-scale solution u^h and multiscale solution u_{ms}^H , respectively.

equation by the finite element method. We do not assume that the function form for the coefficient and source term in micro scale are not known. But we infer them from the coefficients of the given linear system. We explain the detailed procedure how the We tested several numerical examples which confirm the approach proposed in this paper works well for various cases.

Acknowledgment

DS was supported in part by National Research Foundation of Korea (NRF-2017R1A2B3012506 and NRF-2015M3C4A7065662).

References

- [1] A. Abdulle. The finite element heterogeneous multiscale method: A computational strategy for multiscale pdes. *GAKUTO International Series Mathematical Sciences and Applications*, 31(EPFL-ARTICLE-182121):135–184, 2009.
- [2] A. Abdulle, W. E, B. Engquist, and E. Vanden-Eijnden. The heterogeneous multiscale method. *Acta Numerica*, 21:1–87, 2012.
- [3] K. Cho, I. Kim, R. Kim, and D. Sheen. Algebraic multiscale method for two-dimensional elliptic problems. *this journal*, 2002.
- [4] K. Cho and M. Moon. Multiscale hybridizable discontinuous Galerkin method for elliptic problems in perforated domains. *Journal of Computational and Applied Mathematics*, 365:112346, 2020.

- [5] Y. Efendiev, J. Galvis, and T. Y. Hou. Generalized multiscale finite element methods (gmsfem). *Journal of Computational Physics*, 251:116–135, 2013.
- [6] Y. Efendiev and T. Y. Hou. *Multiscale finite element methods: Theory and applications*, volume 4. Springer Science & Business Media, 2009.
- [7] Y. Efendiev, R. Lazarov, M. Moon, and K. Shi. A spectral multiscale hybridizable discontinuous Galerkin method for second order elliptic problems. *Computer Methods in Applied Mechanics and Engineering*, 292:243–256, 2015.
- [8] Y. Efendiev, R. Lazarov, and K. Shi. A multiscale HDG method for second order elliptic equations. Part I. Polynomial and homogenization-based multiscale spaces. *SIAM Journal on Numerical Analysis*, 53(1):342–369, 2015.
- [9] Y. R. Efendiev, T. Y. Hou, and X.-H. Wu. Convergence of a nonconforming multiscale finite element method. *SIAM Journal on Numerical Analysis*, 37(3):888–910, 2000.
- [10] T. Hou, X.-H. Wu, and Z. Cai. Convergence of a multiscale finite element method for elliptic problems with rapidly oscillating coefficients. *Mathematics of Computation of the American Mathematical Society*, 68(227):913–943, 1999.
- [11] C. S. Lee and D. Sheen. Nonconforming generalized multiscale finite element methods. *Journal of Computational and Applied Mathematics*, 311:215–229, 2017.